Segel, I. H. (1976) in *Biochemical Calculations*, pp 309, John Wiley and Sons, New York.
Ugurbil, K. (1985) *J. Magn. Reson. 64*, 207-219.
Verhoeven, J., Kramer, P., Groen, A. K., & Tager, J. M. (1985) *Biochem. J. 226*, 183-192.
Vignais, P. V. (1976) *Biochim. Biophys. Acta 456*, 1-38.
Williamson, J. R., & Corkey, B. E. (1969) *Methods Enzymol. 13*, 434-513.
Zweier, J. L., & Jacobus, W. E. (1987) *J. Biol. Chem. 262*, 8015-8021.

Similarities in Structure between Holocytochrome b_5 and Apocytochrome b_5: NMR Studies of the Histidine Residues†

Cathy D. Moore, Ousaima N. Al-Misky, and Juliette T. J. Lecomte*
Department of Chemistry, The Pennsylvania State University, University Park, Pennsylvania 16802
Received April 1, 1991; Revised Manuscript Received June 13, 1991

ABSTRACT: The properties of the six histidine residues of apocytochrome b_5 have been investigated by using one- and two-dimensional proton NMR spectroscopy in order to probe the structure remaining after heme removal. Spectral assignments were arrived at by analyzing proton NOE connectivities, comparing them to those observed in the holoprotein, and inspecting the X-ray structure of the latter species. Each histidine residue was studied for its pK_a value, interaction with the relaxation agent copper nitrilotriacetic acid, and reactivity toward bromoacetic acid. The four histidines which are not coordinated to the iron atom in the holoprotein (His-15, -26, -27, and -80) display in the major conformer of the apoprotein the same characteristic properties as in the holoprotein. Three of them are involved in specific interactions with the rest of the structure: His-15 and His-80 participate in hydrogen bonds, and His-27 is influenced by the nearby C-terminal segment. His-26 is the most exposed to the solvent. His-63 and His-39, which are located in the heme binding site, have distinct pK_a values; they are affected differently by the copper agent and exhibit comparable reactivity toward bromoacetic acid, albeit milder than that of His-26. The results show that the heme binding residues are clearly distinguishable by their physicochemical properties and that several elements of native holoprotein structure are in place in the apoprotein. It is proposed that the structural influence of the heme is localized and that the amino- and carboxy-terminal segments form a structural unit providing stability to the apoprotein and supporting a fluctuating, partially folded binding site.

The heme-containing, water-soluble fragment of cytochrome b_5 (cyt b_5)[1] is a small globular protein made of both α-helices and β-sheet (Mathews et al., 1971). Its heme prosthetic group is buried in the protein matrix and is known to play an essential role in the definition and stabilization of the structure of the holoprotein (Huntley & Strittmatter, 1972). In order to probe this role, we are currently characterizing physicochemical properties of the apoprotein by nuclear magnetic resonance spectroscopy. We recently reported results demonstrating the presence in the apoprotein of a stable cluster of side chains which overlaps with the second hydrophobic core of the holoprotein (Moore & Lecomte, 1990). This structured region contains the only tryptophan residue, Trp-22, and two of the protein's six histidine residues, His-15 and His-80. In the holoprotein, His-15 and His-80 are found on opposite sides of the β-sheet, form hydrogen bonds with backbone atoms, and are thought to stabilize helices I and VI, respectively (Mathews et al., 1979). The other four histidine residues are located at positions 26, 27, 39, and 63. His-26 and -27 are situated in a turn connecting strands 3 and 4; His-39 and His-63 are the two axial ligands of the iron atom and terminate two of the four helices forming the heme cavity. Thus, the six histidine residues are scattered throughout the protein and provide good markers of structural features. In particular, the two heme pocket histidine residues are expected to report on the state of the vacant binding site.

The assignment of the six histidines in rat liver apocyt b_5 is readily achieved by applying two-dimensional proton NMR techniques. To probe the environment of each residue, acid-base and paramagnetic relaxation agent titrations were performed. Histidine modification studies were also undertaken to determine relative reactivity. The results can be directly compared to those obtained in the holoprotein: the pK_a's of the histidine residues for two different isotypes of cyt b_5, beef and rabbit, are available (Altman et al., 1989) while beef liver cyt b_5 has been titrated with the relaxation agent Cu(NTA)$^-$ for the purpose of electron-transfer studies (Reid et al., 1987). Chemical modification of the histidines using DEP has also been examined (Konopka & Waskell, 1988a,b; Altman et al., 1989).

In this paper, we discuss the properties of the histidine residues of apocyt b_5 as they contribute to a detailed description of the apoprotein. The data continue to show a native holo-

† Supported in part by BRSG Grant S07 RR07082-22 awarded by the Biomedical Research Support Grant Program of the National Institutes of Health and in part by Grant DK 43101 from the National Institutes of Health.
* To whom correspondence should be addressed.

[1] Abbreviations: apocyt b_5, apo form of the water-soluble fragment of cytochrome b_5; CD, circular dichroic; DEP, diethyl pyrocarbonate; COSY, two-dimensional correlated spectroscopy; cyt b_5, water-soluble fragment of cytochrome b_5; DQF-COSY, double-quantum-filtered COSY; holocyt b_5, holo form of the water-soluble fragment of cytochrome b_5; NMR, nuclear magnetic resonance; NOE, nuclear Overhauser effect; NOESY, two-dimensional nuclear Overhauser spectroscopy; NTA, nitrilotriacetic acid; SDS-PAGE, sodium dodecyl sulfate-polyacrylamide gel electrophoresis; TOCSY, total correlation spectroscopy; 2Q, two-quantum spectroscopy.

0006-2960/91/0430-8357$02.50/0

protein-like environment for His-15 and for His-80, extend the similarity to the surroundings of His-26 and His-27, and indicate that the unliganded His-39 and His-63 have properties modulated by their environment. They point to a specific structural and thermodynamic role for the β-sheet and the two helices which are not part of the heme binding site.

Materials and Methods

Materials. Materials for cell growth were obtained from Difco Laboratories. Cell lysis was completed with lysozyme, RNase A, DNase I, dithiothreitol, and *p*-toluenesulfonyl chloride, all purchased from Sigma. The columns used for purification were a DEAE-Sephacel ion exchanger (a Pharmacia product purchased through Sigma) and a Bio-gel P-30 sizing gel (Bio-Rad). Acrylamide, Coomassie brilliant blue dye, and sodium dodecyl sulfate were obtained from Hoefer Scientific Instruments; other materials needed for the SDS–PAGE or the nondenaturing gels came from Aldrich or Sigma. Reagent-grade cupric sulfate pentahydrate and NTA were purchased from Fisher and Kodak, respectively. Bromoacetic acid, approximately 99% pure, was acquired from Sigma, as was the horse skeletal myoglobin used for the neutral heme extraction.

Protein Preparation. The protein used is the soluble fragment of rat liver cyt b_5 expressed from a synthetic gene in *Escherichia coli*, strain TB-1 (Beck von Bodman et al., 1986; the cell line was generously provided by Dr. S. G. Sligar). The cells were grown in LB broth at pH 7.4 and 37 °C in 2-L shaker flasks for approximately 18 h. Cells were harvested by centrifugation, and the reported method for cell lysis and protein purification was followed (Beck von Bodman et al., 1986). The resulting protein appeared as a single band by SDS–PAGE and gave an A_{412}/A_{280} of 5.65. The apoprotein was prepared by using the methyl ethyl ketone method of Teale (1959). Residual holoprotein accounted for less than 1% of the total protein as evaluated by UV–vis spectroscopy. Protein concentrations were evaluated by using $\epsilon_{413} = 114$ mM^{-1} cm^{-1} for the holoprotein and $\epsilon_{280} = 10.6$ mM^{-1} cm^{-1} for the apoprotein (Strittmatter, 1960).

NMR Samples and NMR Methods. Sample concentrations were 1–2 mM for one-dimensional and 2–4 mM for two-dimensional experiments; exchangeable protons were removed by lyophilizing the protein from ^2H_2O once after allowing the protein to exchange overnight at room temperature. ^{1}H NMR spectra were recorded on a Bruker AM-500 spectrometer operating in the quadrature mode at a proton frequency of 500 MHz. The probe temperature was maintained at 298 K. Double-quantum-filtered COSY spectra (Rance et al., 1983) and two-quantum spectra (Braunschweiler et al., 1983; Rance & Wright, 1986) were acquired according to the standard procedure; phase-sensitive NOESY spectra (Kumar et al., 1980; Bodenhausen et al., 1984) were recorded with a Hahn echo (Davis, 1989) and sine modulation in the t_1 domain (Otting et al., 1986). The mixing times ranged from 50 to 200 ms; spin diffusion is noted at mixing times of 150 ms and longer in the 4 mM samples. TOCSY spectra (Braunshweiler & Ernst, 1983; Rance, 1987) were recorded with mixing times of 40 and 75 ms using the DIPSI-2 pulse train (Shaka et al., 1988). Quadrature detection in the ω_1 domain was implemented through the time proportional phase increment method (Drobny et al., 1979; Marion & Wüthrich, 1983). The carrier and decoupler frequencies were phase-coherent and placed on the $^1H^2HO$ line in all two-dimensional experiments (Zuiderweg et al., 1986). The 90° transmitter pulse was 7.4–7.6 μs. Water elimination was achieved by presaturation of the resonance with a 0.75- or 1.2-s decoupler pulse.

DQF-COSY spectra were recorded with a spectral width of 7042 Hz in both dimensions. For the 2Q spectra, a spectral width of 7042 Hz was used in the ω_2 dimension and 14 084 Hz in the ω_1 dimension. The raw data matrices contained 2048 complex points (t_2) × 512 (t_1) points. For the NOESY and TOCSY spectra, a spectral width of 12 500 Hz was used in the ω_2 dimension and 7042 Hz in the ω_1 dimension, yielding a typical data matrix of 4096 complex points (t_2) × 512 (t_1) points. A total of 96 transients were taken for each t_1 value. Data processing was performed with the FTNMR program of Hare Research Inc. on a DEC Microvax II. In the case of the 2Q spectra, the last 400 points of the free induction decays were zeroed to improve the sensitivity, and the ω_2 base line was corrected with a third-order polynomial function. Phase-shifted sine-bell functions were applied in both dimensions. For the NOESY spectra, high-sensitivity transforms were achieved by applying a sine-bell window function with a shift of 22.5° or 45° and zeroing the final 3072 points prior to transformation of the t_2 domain. After transformation, the base line of each file was brought to zero by adding an appropriate constant. The width of the ω_2 domain was reduced to 6250 Hz by keeping the central 2048 complex points. The t_1 domain was zero-filled once to increase the resolution and filtered with a phase-shifted sine-bell window function. All spectra were processed and plotted in the phase-sensitive mode. Chemical shifts are referenced to the $^1H^2HO$ line at 4.76 ppm.

pH Titrations. Solutions of approximately 1 mM apocyt b_5 and oxidized holocyt b_5 were prepared as described above. The pH* was measured with an Ingold slim-body combination electrode and adjusted in an Eppendorf microcentrifuge tube after removal of the sample from the NMR tube; the pH* values reported here are uncorrected meter readings (Meadows, 1972).

The pH* titrations were performed by using two identical samples beginning at approximately pH* 7; the samples were titrated with 2–2.5-μL aliquots of either 0.1 M ^{2}HCl until the protein precipitated in the acidic region at approximately pH* 5, or 0.1 M NaO^{2}H until pH* 9.88 was reached. Spectra were recorded every 0.2 pH unit. The pH* was measured before and after each NMR spectrum was acquired, and the values agreed to within ±0.03 unit, except above pH* 9.1 where they deviated within ±0.05 unit. The resulting chemical shift versus pH curves for the $C^\delta H$ and $C^\epsilon H$ were fitted by a nonlinear least-squares routine using the equation:

$$\delta_i = \delta_{His} + (\delta_{His^+} - \delta_{His})\{10^{n(pK-pH)}/[1 + 10^{n(pK-pH)}]\}$$

where δ_{His} represents the chemical shift of the neutral form (high-pH limit), δ_{His^+} is the chemical shift of the protonated form (low-pH limit), and n is the Hill coefficient (Markley, 1975). In only one case (His-39) was the fit improved by letting n be adjusted by the program; all other n values were therefore fixed to 1.

Paramagnetic Relaxation Agent Titration. A 2.8 mM sample of apocyt b_5 was prepared, and the exchangeable protons were replaced by deuterons as described above. The paramagnetic relaxation agent Cu(NTA)$^-$ was prepared by dissolving approximately 2.5 mg of $CuSO_4 \cdot 5H_2O$ in 1 mL of ^2H_2O; 1.9 mg of NTA was added to the solution, which resulted in a 9.85 mM solution as determined by visible spectroscopy ($\epsilon_{820} = 62$ M^{-1} cm^{-1}; Kirson & Bornstein, 1960). The pH* of the protein solution was adjusted to 6.23, and that of the copper complex was 6.1. In this titration, small aliquots of Cu(NTA)$^-$ were added to the protein solution, and the pH* was checked and adjusted if necessary before the NMR spectrum was acquired. The solution was titrated with the copper complex to a final concentration of about 1 mM, which

Table I: Chemical Shift and pK_a Values for the Histidine Residues of Oxidized Holocytochrome b_5 and Apocytochrome b_5

	chemical shift[a]		pK_a			
proton	apo	holo	apo[b]	holo[b]	holo[c] (beef)	holo[c] (rabbit)
15 ϵ_1	8.07	7.89	8.54 ± 0.02[d]	8.62 ± 0.01[d]		
15 δ_2	6.62	6.76	8.47 ± 0.01[d]	8.73 ± 0.02[d]		
15 av[e]			8.50 ± 0.07	8.68 ± 0.09	8.47	8.38
26 ϵ_1	8.11	8.35	6.93 ± 0.01[d]	6.89 ± 0.02[d]		
26 δ_2	7.00	7.04	6.87 ± 0.02[d,f]	6.85 ± 0.02[d]		
26 av			6.90 ± 0.07	6.87 ± 0.07	6.92	6.91
27 ϵ_1	7.78	7.77	5 < pK_a < 6[g]	5 < pK_a < 6[g]		
27 δ_2	6.88	6.86	5 < pK_a < 6[g]	5 < pK_a < 6[g]		
27 av			5 < pK_a < 6	5 < pK_a < 6	NA[h]	6.44
39 ϵ_1	8.48	NA	7.67 ± 0.01[i]	NA		
39 δ_2	6.84	NA	7.69 ± 0.02[i]	NA		
39 av			7.68 ± 0.07	NA	NA	NA
63 ϵ_1	8.30	NA	7.36 ± 0.01[d]	NA		
63 δ_2	7.17	NA	7.35 ± 0.02[d]	NA		
63 av			7.36 ± 0.07	NA	NA	NA
80 ϵ_1	7.58	7.54	<5.5	<5.5		
80 δ_2	7.00	6.94	<5.5	<5.5		
80 av			<5.5	<5.5	<5.5	<5.0

[a] Apoprotein chemical shifts are reported at pH* 6.88 while holoprotein shifts are given at pH* 6.87; values are accurate to ±0.01 ppm. [b] This work. [c] Determined by Altman et al. (1989). [d] pK_a values (±standard deviation) obtained by fitting the data to a Henderson–Hasselbalch equation with fixed unit Hill coefficient. [e] Average pK_a value for the side chain with estimated error. [f] The last two points at the acidic end (Figure 4B) were omitted from the fit. [g] Lower limit estimate based on reasonable $\delta_{His^+} - \delta_{His}$ values and the observation of an inflection in the C$^\epsilon$H curve. [h] NA, not available. [i] Fitted Hill coefficient of 1.15 ± 0.04.

is where nonspecific broadening is supposed to occur (Roberts & Jardetzky, 1970). The pH* was also checked after each spectrum was acquired; all experiments were within ±0.03 pH unit of 6.23. The widths at half-height of the histidine signals were determined by individual simulation with Lorentzian functions. The line-width increment ($\Delta\nu = \nu - \nu_0$, where ν_0 is the width in the absence of relaxation agent) was then plotted versus copper concentration. The error in the line width increases both with the line width and with the number of copper agent additions (i.e., as overlapping amide signals grow in intensity). Resonance simulation was abandoned when the peak was broadened beyond recognition from the background. No attempt was made to fit the titration profile.

Chemical Modification. The carboxymethylation reaction (Hugli & Gurd, 1970) was carried out for 2 days at room temperature. The reaction mixture was initially 0.326 mM holocyt b_5, 100 mM sodium phosphate buffer, and 200 mM bromoacetic acid, corresponding to a molar ratio of 613:1. Upon addition of the bromoacetic acid to the protein solution, the pH dropped from 7.6 to 7.1 and was maintained at that value for the duration of the reaction. Nondenaturing polyacrylamide gel electrophoresis utilizing a continuous buffer system and a 15% gel was used to monitor the number of histidines modified as a function of time: 50-μL aliquots of the reaction solution were withdrawn at set intervals, and the reaction was quenched by applying the aliquots directly to a Sephadex G-25 column. The remaining modified protein reaction solution was quenched, concentrated by using an Amicon microfiltration system (YM-5 membrane), and exchanged with ^2H_2O in preparation for NMR data collection. A 1-D ^{1}H NMR spectrum was obtained on the resulting sample which was 2.0 mM at pH* 7.04. After this spectrum was acquired, the sample was diluted to 0.65 mM, and the heme was extracted at room temperature for 5 h by adding a 0.734 mM equine apomyoglobin solution prepared by the method of Teale (1959). The pH of the solution was adjusted to 5.98 with 0.1 M HCl, and 23 mg of Tris-HCl was added. The reaction solution was spun down at 10000 rpm for 6 min; the supernatant was applied to a Whatman CM 52 cation-exchange column (50 mM Tris·HCl buffer, pH 6.0). Recovery of apocyt b_5 was 32% with a 6.8% holocyt b_5 impurity, as determined by UV–vis spectroscopy. The solution was concentrated and exchanged with ^2H_2O. The concentration of the resulting NMR sample was 0.88 mM, pH* 6.89.

In situ carboxymethylation was carried out for 20 h at pH* 7.16 using 0.4 mM apocyt b_5 sample in 150 mM phosphate buffer and 200 mM bromoacetic acid, corresponding to a molar ratio of 500. The bromoacetic acid and phosphate buffer were exchanged and lyophilized 3 times with ^2H_2O prior to addition to the apocyt b_5 solution. For NMR data collection, the bromoacetic acid and $^1H^2HO$ resonances were eliminated by saturation with a 4-s and a 1-s decoupler pulse, respectively. At the beginning of each hour of the reaction, spectra consisting of 200 transients were obtained.

Results

Spectral Assignments

(I) Holoprotein. A phase-sensitive NOESY spectrum was recorded with a mixing time of 200 ms to assign the four nonliganded histidine residues of the oxidized rat holoprotein. Connectivities were observed for His-15, -26, and -80 which are consistent both with the solid-state structure (Mathews et al., 1971) and with published beef liver data (Reid et al., 1987). His-27 is not present in the beef protein (Ozols & Heinsemann, 1982) and is assigned by default. The chemical shift values of C$^\delta$H and C$^\epsilon$H at neutral pH are listed in Table I. This assignment procedure is identical with that applied by Altman and co-workers to the rabbit and pig proteins (Altman et al., 1989). Native rat liver cyt b_5 is a mixture of two heme rotational isomers (Rodgers et al., 1988; Pochapsky et al., 1990). Chemical shifts are reported only for the major form.

(II) Apoprotein. Histidine ring resonances are readily identified in 2Q experiments (Dalvit et al., 1987). Figure 1A shows the relevant section of a 2Q spectrum recorded on the rat apoprotein in ^2H_2O at pH* 6.14 with a mixing time of 80 ms. The sharp resonances of the six histidines are clearly resolved and the expected C$^\delta$H–C$^\epsilon$H cross-peaks detected. The labels in Figure 1A were derived from the analysis of NOESY spectra as explained below. The chemical shifts of C$^\delta$H and C$^\epsilon$H of the six His rings are listed in Table I along with the holoprotein values.

(A) His-15 and His-80. His-15 has been previously assigned on the basis of dipolar contacts with Trp-22, a residue which

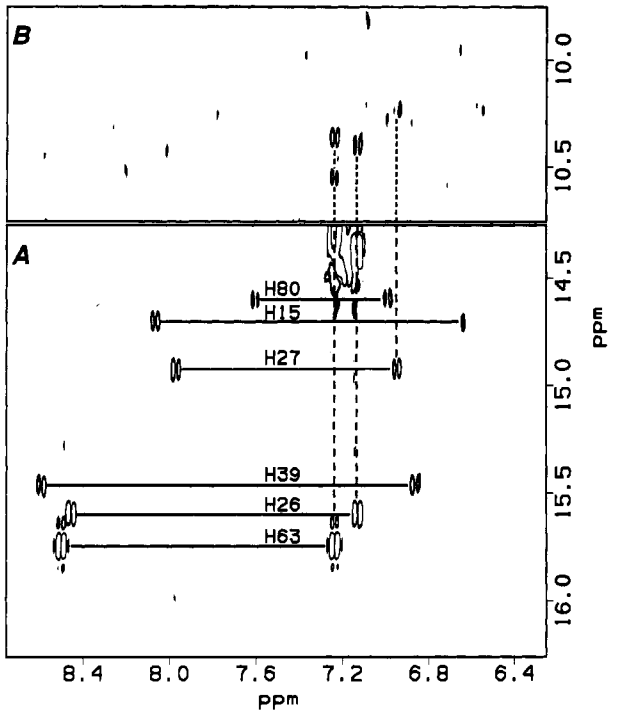

FIGURE 1: Two-quantum spectrum of apocytochrome b_5 recorded at 500 MHz in ^2H_2O at pH* 6.14, 298 K. Positive and negative levels are plotted without distinction. (A) Connectivities between $C^\delta H$ and $C^\epsilon H$; (B) connectivities between $C^\delta H$ and $C^\beta H$ of histidine residues. Assignments are discussed in the text.

is involved in similar local structure both in the apoprotein and in the holoprotein (Moore & Lecomte, 1990). In the same work, a weak NOE to the ring of Tyr-6 was used to identify the side chain of His-80. Additional NOE connectivities can be analyzed to extend the characterization of the environment of His-80. For example, Figure 2A contains a region of a phase-sensitive NOESY spectrum (τ_m = 100 ms, ^2H_2O) which illustrates the proximity of the $C^\delta H$ to a methyl group at 1.2 ppm. TOCSY spectra (τ_m = 75 ms) identify the side chain as a threonine with $C^\beta H$ at 4.85 ppm, $C^\alpha H$ at 4.59 ppm, and NH at 9.33 ppm. NOESY data collected in 90% ^1H_2O/10% ^2H_2O locate this threonine NH near the $C^\alpha H$ of Tyr-7 at 5.18 ppm and thus point to Thr-8. Furthermore, His-80 $C^\epsilon H$ is close to an amide proton resonating at 11.12 ppm. The corresponding $C^\alpha H$ is identified at 4.44 ppm (DQF-COSY spectrum), and the $C^\beta H$'s are centered at 2.63 ppm (TOCSY spectrum). The latter pair of protons is also located near the $C^\epsilon H$ of His-80. In accordance with the X-ray structure and holoprotein data (Veitch et al., 1988; Guiles et al., 1990), assignment of this side chain is made to Asp-82.

(*B*) *His-26 and -27.* These two residues are assigned through backbone $C^\alpha H_i - NH_{i+1}$ and side-chain connectivities which delineate a Leu-His-His sequence (Leu-25, $C^\alpha H$ at 4.56 ppm and NH at 9.13 ppm; His-26, $C^\alpha H$ at 3.96 ppm and NH at 9.39 ppm; His-27, $C^\alpha H$ at 4.08 ppm and NH at 8.51 ppm). It is interesting to note that the $C^\delta H$'s of both His-26 and His-27 display connectivities to one of their $C^\beta H$'s in the 2Q spectrum (Figure 1B). These correlation cross-peaks confirm the assignment of the corresponding $C^\alpha H$'s. In addition, the $C^\delta H$ of His-26 shows medium NOEs to both $C^\delta H_3$'s of Leu-25 (0.24 and 0.61 ppm) and its $C^\gamma H$ (1.16 ppm) (Figure 2A). One of the $C^\delta H_3$'s of Leu-25 presents medium NOEs to the ring of Tyr-30 (Figure 2A) as seen in the holoprotein spectrum. His-27 shows several NOEs to the aliphatic region of the spectrum, but most relevant to this work is the effect observed from the $C^\delta H$ proton to a $C^\alpha H$ at 3.94 ppm which can be

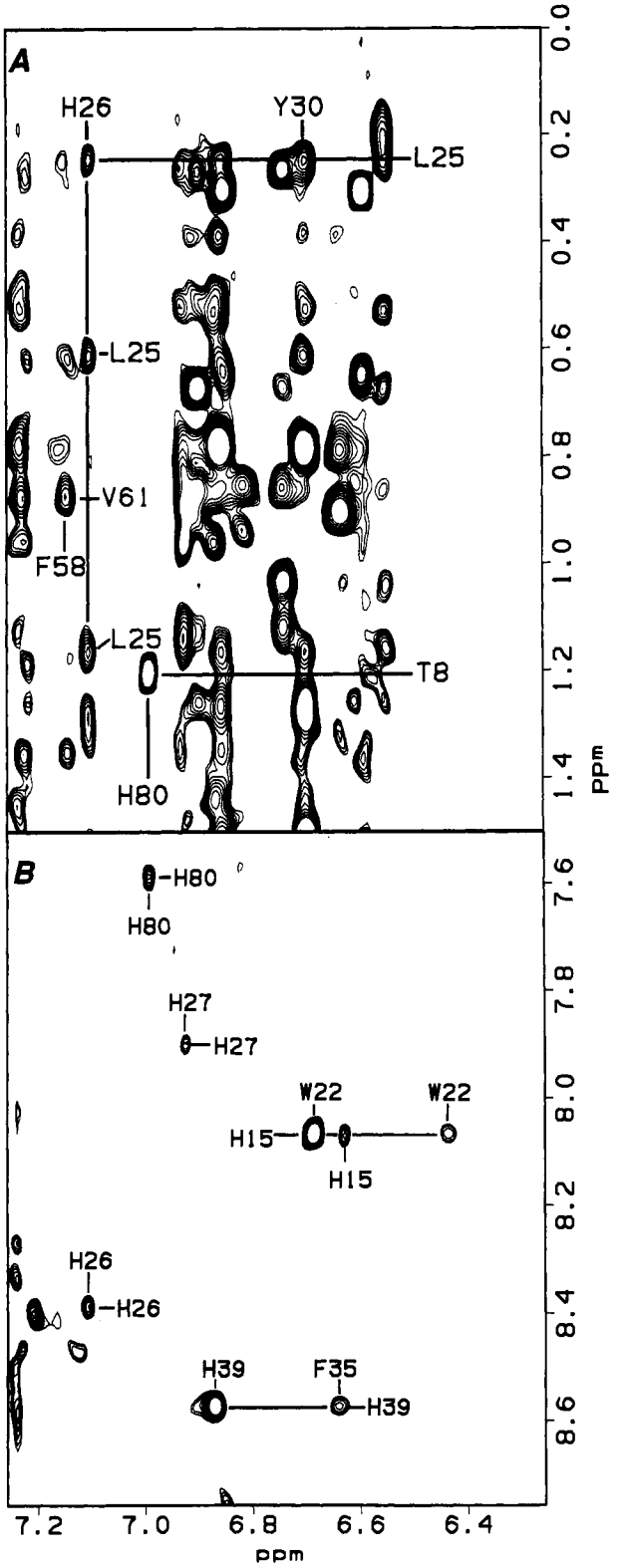

FIGURE 2: NOESY spectrum of a 4 mM sample of apocytochrome b_5 at pH* 6.11 and 298 K recorded in ^2H_2O with a mixing time of 100 ms. (A) Aliphatic/aromatic connectivities. (B) His $C^\epsilon H$/aromatic connectivities.

assigned to Arg-84 based on backbone connectivities starting from Asp-82.

(*C*) *His-39.* A 2Q spectrum recorded with a mixing time of 25 ms locates the $C^\delta H$'s of Phe-35 at 6.63 ppm. These protons have a medium-size NOE to the $C^\epsilon H$ of a histidine residue at 8.55 ppm (Figure 2B). In the holoprotein crystal structure, the ring of Phe-35 is located fewer than 6 Å from

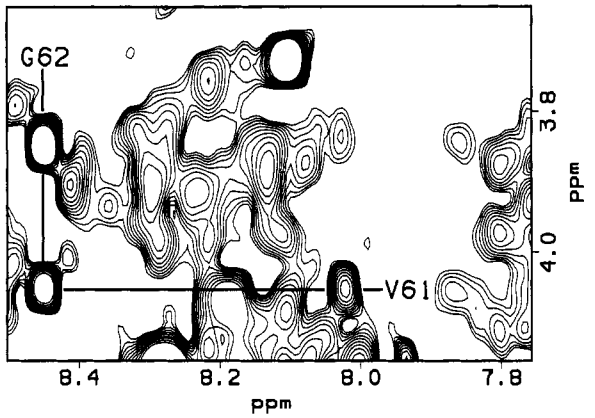

FIGURE 3: NOESY spectrum of a 4 mM sample of apocytochrome b_5 at pH 6.5 and 298 K recorded in 90% ^1H_2O/10% ^2H_2O with a mixing time of 75 ms. The region contains NOE cross-peaks between $C^\alpha H$ and NH of residues Val-61 and Gly-62.

that of His-39 (Mathews et al., 1979). All other histidines are located farther away. Thus, although structural perturbations are expected in this region of the protein, the histidine in contact with Phe-35 is assigned as His-39.

(*D*) *His-63.* The remaining histidine, His-63, is on the opposite side of the heme binding site. The $C^\delta H$ shows NOEs to the $C^\alpha H$ at 4.71 ppm and the $C^\beta H$'s at 3.31 and 3.12 ppm. These assignments are confirmed by strong $C^\delta H$–$C^\beta H$ connectivities in the 2Q spectrum (Figure 1B). In the holoprotein, the direct environment of His-63 includes Phe-58 and Val-61. In the apoprotein, Phe-58 has practically no interresidue NOEs at mixing times up to 75 ms. At longer mixing times, NOEs to Leu-25 and to the sharp and degenerate $C^\gamma H_3$'s of a valine residue at 0.88 ppm are observed (Figure 2A). TOCSY spectra place the $C^\alpha H$ of the valine at 4.05 ppm and its NH at 8.02 ppm. Pertinent backbone connectivities are illustrated in Figure 3: the amide proton of the valine is in dipolar contact with a residue whose $C^\alpha H$ is at 3.85 ppm. A remote connectivity at ω_2 = 8.45 ppm and ω_1 = 7.70 ppm in the 2Q spectrum (τ_m = 25 ms) identifies the latter as a glycine with degenerate $C^\alpha H$'s. This Val-Gly connectivity assigns Val-61 and Gly-62. The $C^\alpha H$ of His-63 is at 4.71 ppm and is saturated along with the H_2O signal in the 90% H_2O samples; thus, backbone NOE connectivities are interrupted at Gly-62.

In the course of our analysis of NMR data, we also have found a number of cross-peaks indicative of conformational exchange, slow on the NMR time scale (J. T. J. Lecomte and C. D. Moore, unpublished results). The equilibrium affects the region of the structure containing His-80 and His-27. However, the non-hololike conformers account for a small proportion of the total apoprotein (<10%), and in this paper, we limit our discussion to the major, hololike form.

pH Titration

Figure 4 shows plots of the pH titration curves for the ring protons of the six histidines in the apoprotein and of the four non-heme-bound histidines of the major isomer of the oxidized holoprotein. Titration of the apoprotein and the holoprotein ended at pH 5.3 and 5.0, respectively, as below these pH values the protein begins to precipitate. The high-pH limits were 9.9 (apoprotein) and 9.8 (holoprotein). The pK_a values obtained by fitting the data to a Henderson–Hasselbalch equation are listed in Table I. $C^\delta H$ and $C^\epsilon H$ of all the histidines in the apoprotein and holoprotein exhibit the same pK_a value within experimental error; only the $C^\epsilon H$ of His-26 deviates from the behavior predicted by the equation.

His-15 has a pK_a of 8.5 in the apoprotein and 8.7 in the holoprotein (Figure 4A), values which are high compared to

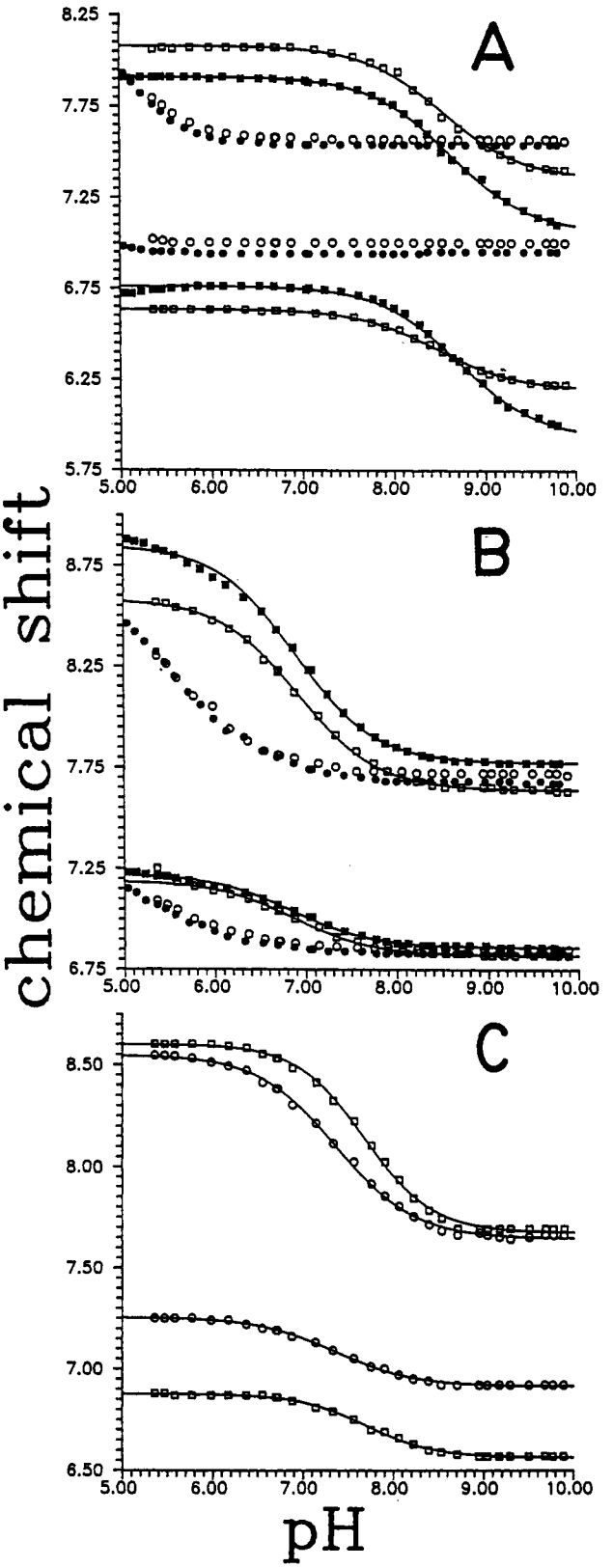

FIGURE 4: Plots of chemical shift in ppm versus pH for $C^\delta H$ and $C^\epsilon H$ of histidine residues in rat liver cytochrome b_5. Closed symbols represent oxidized holoprotein data; open symbols represent apoprotein data. (A) His-15 (□) and His-80 (○); (B) His-26 (□) and His-27 (○); (C) His-39 (□) and His-63 (○). The lines through the data points were calculated by applying a Henderson–Hasselbalch equation with parameters as described in Table I.

the pK_a of ≈6.6 for a freely titrating histidine residue (McNutt et al., 1990). In contrast, the ring proton chemical shifts of His-80 remain constant above pH 6 in both the apo- and

holoprotein; pH 6 marks the onset of the titration (Figure 4A). Since the protein precipitates before the low-pH plateau can be reached, the pK_a value of this residue could not be determined, and an upper limit of 5.5 is proposed. One of the two adjacent histidines, His-26, shows a pK_a value of 6.90, close to that of a freely accessible histidine and independent of the presence of the heme (Figure 4B). The other, His-27, has no well-defined low-pH plateau, and its pK_a is estimated to lie between 5 and 6. It also appears independent of the presence of the heme (Figure 4B). The low pK_a and the NOEs observed to the ring imply that this residue, unlike His-26, is engaged in specific interactions with the rest of the protein. The heme binding residues, His-39 and His-63, have distinct pK_a values of 7.68 and 7.35, respectively (Figure 4C). The acidities point to differences in the environment of the two histidines normally coordinated to the iron atom.

The resonances for the nontitrating groups of apocyt b_5 shift moderately as the pH is changed. Among the assigned signals, the $C^{\delta}H_3$ of Ile-76 experiences the largest perturbation, moving from −0.95 ppm to −0.71 ppm. The upfield shift from the random-coil value is due to the ring current generated by Trp-22 and makes this resonance diagnostic of the presence of the second hydrophobic core (Keller & Wüthrich, 1980; Moore & Lecomte, 1990). Similar shifts in the resonance position of other residues involved in the hydrophobic core (Trp-22, Tyr-7, and Val-29) are also observed. In the methyl region of apocyt b_5, a sharp doublet resonating at 1.5 ppm at neutral pH titrates with an apparent pK_a of about 8.5 (not shown). This resonance corresponds to the methyl protons of an alanine residue. No NOE is observed to His-15 (which has the same pK_a value) or its neighbors, and assignment is tentatively made to the N-terminal alanine. The apparent pK_a is consistent with that of protein amino termini ($pK_a \approx 8.0$; Stryer, 1988).

Cu(II) Titration

Shown in Figure 5A are one-dimensional spectra representative of the titration of a 2.8 mM apocyt b_5 solution with a 9.25 mM $Cu(NTA)^-$ solution. The results are summarized by a plot of the change in line width versus relaxation agent concentration for the six histidine $C^{\epsilon}H$ resonances (Figure 5B). Upon addition of the copper solution to a concentration of 0.1 mM, the resonances of His-26 are affected first, followed closely by those of His-27 and His-63. For these three residues, the effect is noticeable at 0.25 mM (Figure 5A, trace b). It is not until higher concentrations are reached that His-39 is significantly affected and greater still that His-80 and His-15 broaden to an appreciable extent. Difference spectroscopy reveals that the resonances of Phe-58 broaden at approximately the same concentration of Cu^{2+} as those of His-63 do; this agrees well with the observed NOE data which indicate proximity of the two residues in the apoprotein. Other aromatic residues, Tyr-30, Tyr-6, and Phe-35, broaden with His-39 and are therefore characterized by a similar degree of accessibility to the reagent. At approximately 1 mM copper, relaxation of the Tyr-7 and His-15 protons begins to accelerate; these residues are within NOE contact of Trp-22 which is buried in the hydrophobic core of the apoprotein. Trp-22 and Ile-76 are practically unaffected by copper addition over the concentration range explored.

Chemical Modification

The carboxymethylation of histidine residues in the oxidized holoprotein was monitored by native gel electrophoresis which shows a succession of bands corresponding to the addition of a charge as a histidine is modified. The reaction modifies three

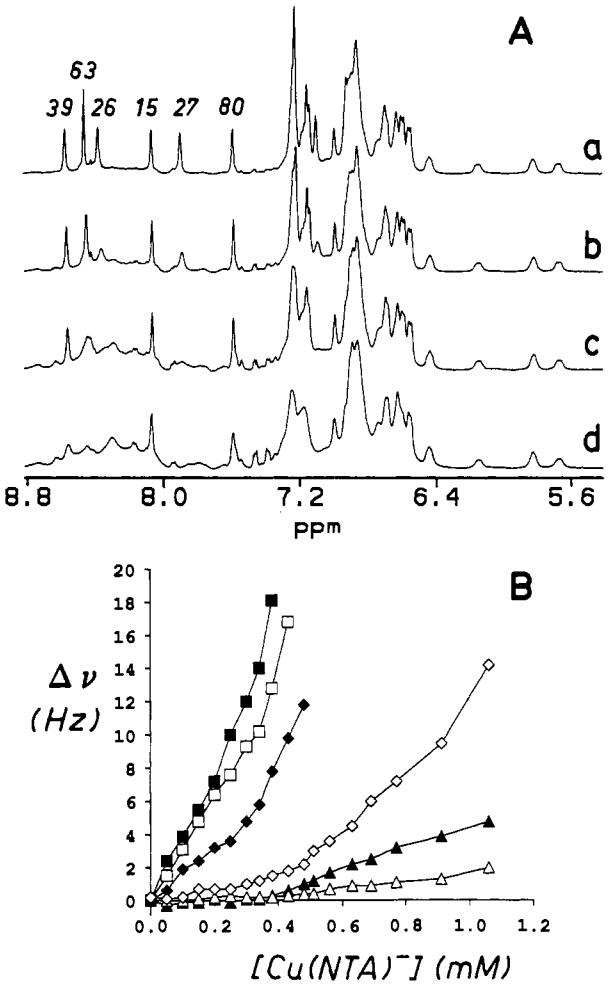

FIGURE 5: Titration of apocytochrome b_5 with the relaxation agent $Cu(NTA)^-$. The titration was performed in ^2H_2O at pH* 6.23 and 298 K. The starting concentration of apocytochrome b_5 was 2.8 mM, and the concentration of the relaxation agent varied from 0 to 1 mM. (A) Representative one-dimensional spectra of the aromatic region as a function of the concentration of added $Cu(NTA)^-$; (a) reference; (b) 0.25 mM; (c) 0.51 mM; (d) 1.06 mM. (B) Plot of line-width increment versus $Cu(NTA)^-$ concentration for the histidine $C^{\epsilon}H$ resonances: (■) His-26; (□) His-27; (♦) His-63; (◇) His-39; (▲) His-80; (△) His-15. Data points are connected to guide the eye.

of the four nonliganded histidine residues in 2 days; His-39 and -63 are not expected to be modified as long as the heme remains bound. The one-dimensional NMR spectrum of the protein after 48 h of reaction demonstrates that the modified His residues are His-26, -27, and -15, although His-15 does not react completely. His-80 is not modified to any measurable extent. To verify the consistency of the histidine assignments, apocyt b_5 was prepared from the reacted holoprotein. In this case, the heme must be extracted under neutral instead of acidic conditions so as not to reverse the histidine modification. This is readily achieved by adding horse apomyoglobin to the cytochrome solution. Horse apomyoglobin, which has a higher affinity for the heme than apocyt b_5, binds the heme and can be removed by cation-exchange chromatography. The spectrum of the apoprotein prepared from modified holoprotein (not shown) is clearly missing the signals from His-26 and -27; His-15 is reduced in intensity, and His-80 is intact.

The carboxymethylation reaction was performed directly on the apoprotein in order to probe the reactivity and accessibility of the histidines in that structure. The intensity of each $C^{\epsilon}H$ signal was monitored as a function of time over a period of 20 h. Figure 6 contains the spectrum of apocyt b_5 1 h after the addition of bromoacetic acid, where little reaction has

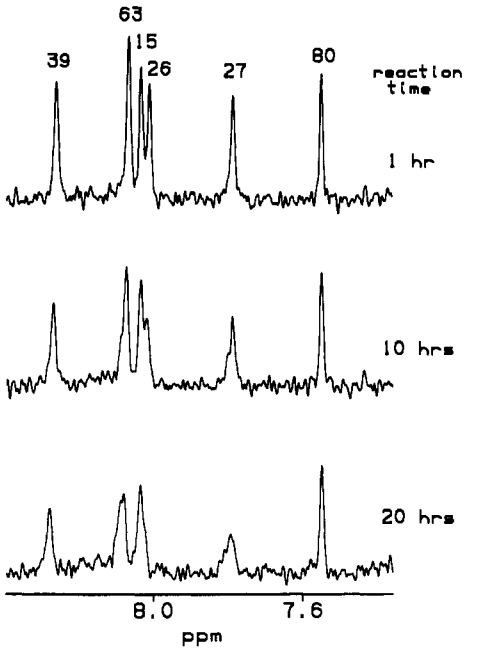

FIGURE 6: One-dimensional spectra of the His $C^{\epsilon}H$ resonances of apocytochrome b_5 as a function of reaction time with bromoacetic acid. The carboxymethylation was performed at pH* 7.2 and 298 K in the presence of 150 mM sodium phosphate buffer and 200 mM bromoacetic acid with a 0.4 mM protein solution. Times plotted are 1, 10, and 20 h after addition of the acid. Note the shoulders in the last spectrum which are thought to arise from product formation.

occurred. Typical spectra obtained after 10 and 20 h of reaction at 298 K are shown below. From data collected every hour, the following reactivity order is obtained: His-26 ≈ His-27 > His-63 ≈ His-39 > His-15 > His-80. Histidines-26, -27, -63, and -39 react rapidly, showing signs of modification within 8 h. His-15 is intermediate in its reactivity, requiring at least 12 h before displaying any detectable decrease in intensity. Under the conditions used, His-80 remains intact for the 20 h that were monitored. Quantitative interpretation of the data is prevented by the growing amount of products in the same region of the spectrum as evidenced by shoulders to the signals of unreacted imidazole groups.

Discussion

Under native conditions, apocyt b_5 is thought to fold into a conformation distinct from that of the holoprotein (Huntley & Strittmatter, 1972). The nature and extent of the differences cannot be determined from the CD data analysis alone, and alternative methods are required to probe the structure. Fluorescence studies (Huntley & Strittmatter, 1972) and NMR studies (Moore & Lecomte, 1990) agree that a major rearrangement does not occur for the buried tryptophan and its surroundings. This residue is located in a nonpolar core, and as a consequence, the packing of hydrophobic residues has been proposed to contribute to the stability of the apoprotein. In this work, we have chosen to characterize the properties of the histidine residues for two main purposes: to define the role of the heme in attaining the functional conformation and to investigate the determinants of stability in the apoprotein.

His-15 and His-80. The hydrophobic core which has been identified in both the apo- and holoprotein is preserved through the extreme pH conditions examined here. Its stability as a function of pH is evidenced by the small shift for the resonances corresponding to Ile-76, Trp-22, Val-29, and Tyr-7 and is attributed to efficient packing of these hydrophobic residues. His-15 and His-80 are located near this core. The pH titration behavior of the histidine residues of holocyt b_5 has been determined by Altman and co-workers (Altman et al., 1989); their results showed that His-15 and -80 have abnormal pK_a's comparable to those we observe in the rat holo- and apoprotein (see Table I). In the case of His-15, the elevated value is thought to be due to a hydrogen bond between the proton of the δ-nitrogen and the backbone carbonyl of Gln-11. The pK_a shift of ≈1.9 units corresponds to an interaction energy of ≈2.6 kcal mol^{-1} at 298 K. The low pK_a value obtained for His-80 has been ascribed to participation of the δ-nitrogen in a hydrogen bond with the amide NH of Asp-82 and corresponds to a free energy of interaction greater than 1.5 kcal mol^{-1}. Both these hydrogen bonds appear conserved in the major conformer of the apoprotein over the pH range 6.0–8.0.

The results of the carboxymethylation reaction and the copper titration are also similar to holoprotein data. Altman and co-workers (Altman et al., 1989) have used DEP to probe the reactivity of the histidines in the beef and rabbit holoprotein; they observed that His-80 is resistant to the reagent whereas His-15 has a moderate reactivity. The reactivity toward bromoacetic acid is expected to depend upon the same factors as that toward DEP: hydrogen-bonding status of the imidazole nitrogens, accessibility to reagent, and pK_a value. Indeed, we find the same modification pattern for the carboxymethylation of rat liver holocyt b_5, His-15 being only partially modified and His-80 not reacting after 2 days in the presence of the reagent. The same relative rates are observed with the apoprotein. The effect of low $Cu(NTA)^-$ concentration on the spectrum of the beef holoprotein has been described (Reid et al., 1987); the resonances of His-15 and -80 broaden at higher concentrations of the reagent than are necessary for His-26. In the rat apoprotein, His-15 and His-80 maintain a narrow line width up to 1 mM $Cu(NTA)^-$ while His-26 is affected at 0.1 mM $Cu(NTA)^-$. Thus, it is concluded on the basis of spectral properties and the results of pH titration, carboxymethylation, and titration with copper that the holoprotein local structure surrounding His-15 and His-80 is maintained in the major conformer of apocyt b_5.

His-26 and His-27. His-26 is the least distinctive of the six histidine residues. Its pK_a value is indicative of exposure to the solvent and is independent of the presence of the heme and the species of origin (Altman et al., 1989). His-26 reacts the fastest with DEP (Altman et al., 1989) and bromoacetic acid, both in the rat holo and in the apo forms (this work); it is also the residue which displays the effect of the copper reagent at the lowest concentration, regardless of the presence of the heme. $Cu(NTA)^-$ is known to bind the beef holoprotein in the region of His-26 and Tyr-27 and to promote the long-range Fe(II) to Cu(II) electron transfer (Reid et al., 1987). In the rat protein, the site and its properties appear unaltered by heme removal.

The case of His-27 is more complex. The pK_a value reported for the rabbit holoprotein is 6.44 (Altman et al., 1989) and contrasts with our estimate (<6.0). Altman and co-workers used a cyt b_5 isolated from the liver and prepared by trypsin solubilization. It comprises residues 3–84. The rat liver protein investigated here, which is expressed from a synthesized gene (Beck von Bodman et al., 1986), contains several additional amino acids: 6 at the amino terminus and 10 at the carboxy terminus. The X-ray structure of beef cyt b_5 (lipase-solubilized, containing residues 1–93) places the C-terminal helix near position 27 in contact with Arg-84 (Mathews et al., 1979). When the protein is cleaved after residue 84, it is likely that the environment of His-27 is altered, perhaps allowing greater exposure to the solvent. Thus, we attribute the discrepancy in the pK_a value in the holoprotein to the truncation of the helix

which normally extends from residue 80 to 87 and docks near position 27. The proximity of residues 27 and 84 in the rat protein is supported by NOEs between the ring of His-27 and the $C^{\alpha}H$ of Arg-84; the presence of a positive charge near the imidazole group could account for the destabilization of the protonated form and the lowered pK_a. The deviation from simple two-state behavior exhibited by the $C^{\epsilon}H$ of His-26 (Figure 4B) may be the result of electrostatic interactions between the rings of His-26 and His-27.

Since the variable length of the polypeptide chain may affect the properties of His-27, the comparison must be limited to the rat holoprotein, and we simply note that the low pK_a of this residue is maintained in the absence of the heme. Carboxymethylation of His-27 occurs rapidly whether the heme is present or not; this observation is consistent with the low concentration of copper reagent required to broaden the line. Hence, as in the case of His-15 and -80, all the tested properties concur to qualify the 26–27 region of the major apoprotein conformer as stable and hololike.

His-39 and His-63. The unliganded His-39 and -63 do not share the same chemical properties: they are characterized by unique pK_a values and by differential line broadening in the presence of the paramagnetic relaxation agent. In addition, they react with bromoacetic acid more slowly than the freely exposed His-26 and give rise to a small number of weak interresidue NOEs. These observations can be used to describe the vacated binding site. They suggest that the segments normally defining the heme pocket are not in a statistical conformation which would expose both imidazole rings to the solvent. They also rule out hydrophobic collapse into a tight core minimizing the surface area of aliphatic and aromatic moieties in contact with water and sequestering the histidines from solvent. Instead, our data are consistent with the formation of a somewhat compact and fluctuating structure with constraints retarding reagent approach and dynamics unfavorable to the detection of NOEs.

The structural characteristics of this region of the protein are yet to be determined. The $Cu(NTA)^-$ titration data suggest that His-63 has a larger accessibility to solvent than His-39. This is in agreement with the static accessibilities calculated for beef holocyt b_5 (Konopka & Waskell, 1988a) and may indicate that the binding site exhibits hololike steric features. However, we note that $Cu(NTA)^-$ is negatively charged. The primary structure of cyt b_5 contains 10 glutamic acid and aspartic acid residues between positions 37 and 66; these, if rearranged, could generate electrostatic interactions accounting for the pK_a values, broadening with copper ions, and reactivity with bromoacetic acid. A detailed analysis of NOE connectivities will aid in assessing the steric and electrostatic contributions. At this point, we stress that His-39 and His-63 exhibit chemical properties which are clearly distinct from those of the other histidine residues in the apoprotein, including the only fully exposed one. It is possible that this uniqueness plays a role in the process of heme recognition and binding.

Histidine residues are sensitive probes of the structure of cyt b_5 because they are under distinct influences generated by the protein matrix. The analysis of their properties has provided us with insight into stabilizing factors of the apoprotein. In the holoprotein, His-15 and -80 are involved in side-chain-to-main-chain hydrogen bonds at the end of helix I and the start of helix VI. These interactions are in place in the apoprotein. His-26 and His-27 maintain their holoprotein properties as well; they point to the formation of the loop linking β strands 3 and 4 and the docking of the last helix. Overall, the four unliganded residues are remarkably unaffected by the prosthetic group. Taken with the data presented previously on the second hydrophobic core (Moore & Lecomte, 1990), the interactions which dictate the histidine behaviors give strong evidence for the correct relative spatial arrangement of four of the five β strands and the two helices which are not a part of the heme pocket. Since apocyt b_5 retains holoprotein structural integrity in the region remote from the binding site, the major perturbations caused by the deletion of interactions between protein matrix and prosthetic group appear confined to the heme cavity.

The emerging picture is that of a partially disorganized structure at the binding site juxtaposed to an organized native region. Thus, in a globular system as small as cyt b_5, the polypeptide can be found in a state intermediate between fully folded and fully denatured. Unfolding of cyt b_5 has been described by Tajima and co-workers, who performed chemical denaturation experiments on the rabbit protein (Tajima et al., 1976). The optical properties they chose to monitor as functions of guanidine hydrochloride reflect heme attachment (absorption spectroscopy in the Soret band at 413 nm) and secondary structure (ellipticity at 222 nm). For the holoprotein, the unfolding process is cooperative and concomitant with heme release. Pfeil and Bendzko (1980) studied the thermal denaturation of the same protein; in addition to the secondary structure, they probed the tertiary structure by evaluating the degree of aromatic residue exposure to solvent (ellipticity at 297 nm). Loss of structure coincides with heme release, and the process follows a simple two-state behavior without stable intermediates. Thus, the denaturation data reinforce that the native hololike structure in apocyt b_5 cannot subsist under the transition midpoint conditions of the holoprotein. To our knowledge, little direct information is available on the unfolding of the apoprotein except for an interesting response to chemical denaturant: the ellipticity at 222 nm changes gradually as the concentration of guanidine hydrochloride increases, in sharp contrast to the holoprotein behavior (Tajima et al., 1976). It is possible that removal of the heme populates a number of additional conformations and that the unfolding of the apoprotein is a multistate process. A study of the thermal and chemical denaturations of rat liver cyt b_5 may elucidate this point and provide an estimate of the contribution of the native structure to the stability.

The existence in the apoprotein of a stable structure with tertiary interactions geometrically and energetically characteristic of the holoprotein raises the hypothesis that the β-sheet and helices I and VI act as an independent structural unit. In the formation of a functional *b* heme protein, a binding site has to be created with the necessary flexibility and recognition capabilities to allow for ready insertion and retention of the appropriate molecule. In addition, the apoprotein must be sufficiently stable for survival in its environment and must be commited to produce the native holoprotein efficiently. The prevention of untimely proteolytic digestion and aggregation is particulary important in the cases where heme insertion lags behind apoprotein synthesis (Shawver et al., 1984). A pathway proceeding through a partly folded precursor accomplishes two goals. The folded native unit provides stability toward degradation and physical stresses and retards precipitation by protecting hydrophobic side chains from the solvent. It also constitutes a support onto which the binding site can be partially shaped and maintained in a fluctuating state. Upon encounter with the prosthetic group, the folding can be rapidly completed without requiring major structural rearrangement except around the bound molecule. Cyt b_5 is probably not

unique in this regard and suggests a mechanism by which larger, complex systems associated with more than one prosthetic group or cofactor adopt their native structure.

ACKNOWLEDGMENTS

We thank Professor Stephen G. Sligar for the gift of cytochrome b_5 gene and continuous encouragement, Dr. Karla Rodgers for advice with the protein preparation, and Drs. Christopher Falzone and C. Robert Matthews for helpful discussions.

REFERENCES

Altman, J., Lipka, J. J., Kuntz, I. D., & Waskell, L. (1989) *Biochemistry 28*, 7516–7523.

Beck von Bodman, A., Schuler, M. A., Jollie, D. R., & Sligar, S. G. (1986) *Proc. Natl. Acad. Sci. U.S.A. 83*, 9443–9447.

Bodenhausen, G., Kogler, H., & Ernst, R. R. (1984) *J. Magn. Reson. 58*, 370–388.

Braunschweiler, L., & Ernst, R. R. (1983) *J. Magn. Reson. 53*, 521–528.

Braunschweiler, L., Bodenhausen, G., & Ernst, R. R. (1983) *Mol. Phys. 48*, 535–560.

Dalvit, C., Wright, P. E., & Rance, M. (1987) *J. Magn. Reson. 71*, 539–543.

Davis, D. G. (1989) *J. Magn. Reson. 81*, 603–607.

Drobny, G., Pines, A., Sinton, S., Weitekamp, D. P., & Wemmer, D. (1979) *Symp. Faraday Soc. 13*, 49–55.

Guiles, R. D., Altman, J., Lipka, J. J., Kuntz, I. D., & Waskell, L. (1990) *Biochemistry 29*, 1276–1289.

Hugli, T. E., & Gurd, F. R. N. (1970) *J. Biol. Chem. 245*, 1939–1946.

Huntley, T. E., & Strittmatter, P. (1972) *J. Biol. Chem. 247*, 4641–4647.

Keller, R. M., & Wüthrich, K. (1980) *Biochim. Biophys. Acta 621*, 204–217.

Kirson, B., & Bornstein, R. (1960) *Bull. Soc. Chim. Fr.*, 288–293.

Konopka, K., & Waskell, L. (1988a) *Arch. Biochem. Biophys. 261*, 55–63.

Konopka, K., & Waskell, L. (1988b) *Biochim. Biophys. Acta 954*, 189–200.

Kumar, A., Ernst, R. R., & Wüthrich, K. (1980) *Biochem. Biophys. Res. Commun. 95*, 1–6.

Marion, D., & Wüthrich, K. (1983) *Biochem. Biophys. Res. Commun. 113*, 967–974.

Markley, J. (1975) *Acc. Chem. Res. 8*, 70–80.

Mathews, F. S., Argos, P., & Levine, M. (1971) *Cold Spring Harbor Symp. Quant. Biol. 36*, 387–395.

Mathews, F. S., Czerwinski, E. W., & Argos, P.(1979) in *The Porphyrins* (Dolphin, D., Ed.) Vol. 7, pp 107–147, Academic Press, New York.

McNutt, M., Mullins, L. D., Raushel, F. M., & Pace, C. N. (1990) *Biochemistry 29*, 7572–7576.

Meadows, D. H. (1972) *Methods Enzymol. 26*, 638–653.

Moore, C. D., & Lecomte, J. T. J. (1990) *Biochemistry 29*, 1984–1989.

Otting, G., Widmer, H., Wagner, G., & Wüthrich, K. (1986) *J. Magn. Reson. 66*, 187–193.

Ozols, J., & Heinsemann, F. S. (1982) *Biochim. Biophys. Acta 704*, 163–173.

Pfeil, W., & Bendzko, P. (1980) *Biochim. Biophys. Acta 626*, 73–78.

Pochapsky, T. C., Sligar, S. G., McLachlan, S. J., & La Mar, G. N. (1990) *J. Am. Chem. Soc. 112*, 5258–5263.

Rance, M. (1987) *J. Magn. Reson. 74*, 557–564.

Rance, M., & Wright, P. E. (1986) *J. Magn. Reson. 66*, 372–378.

Rance, M., Sørensen, O. W., Bodenhausen, G., Wagner, G., Ernst, R. R., & Wüthrich, K. (1983) *Biochem. Biophys. Res. Commun. 117*, 479–485.

Reid, L. S., Gray, H. B., Dalvit, C., Wright, P. E., & Saltman, P. (1987) *Biochemistry 26*, 7102–7107.

Roberts, G. C. K., & Jardetzky, O. (1970) *Adv. Protein Chem. 24*, 447–545.

Rodgers, K. K., Pochapsky, T. C., & Sligar, S. G. (1988) *Science 240*, 1657–1659.

Shaka, A. J., Lee, C., & Pines, A. (1988) *J. Magn. Reson. 77*, 274–293.

Shawver, L. K., Seidel, S. L., Krieter, P. A., & Shires, T. K. (1984) *Biochem. J. 217*, 623–632.

Strittmatter, P. (1960) *J. Biol. Chem. 235*, 2492–2497.

Stryer, L. (1988) in *Biochemistry* 3rd ed., p 21, Freeman, New York.

Tajima, S., Enomoto, K.-I., & Sato, R. (1976) *Arch. Biochem. Biophys. 172*, 90–97.

Teale, F. W. J. (1959) *Biochim. Biophys. Acta 35*, 543.

Veicht, N. C., Concar, D. W., Williams, R. J. P., & Whitford, D. (1988) *FEBS Lett. 238*, 49–55.

Zuiderweg, E. R. P., Hallenga, K., & Olejniczak, E. T. (1986) *J. Magn. Reson. 70*, 336–343.